Supporting Information for

Facile and scalable synthesis of $Zn_3V_2O_7(OH)_2·2H_2O$ microflowers as a high-performance anode for lithium-ion batteries

Haowu Yan,[†] *Yanzhu Luo,*[*,†,‡] *Xu Xu,*[†] *Liang He,*[†,§] *Jian Tan,*[†] *Zhaohuai Li,*[†] *Xufeng Hong,*[†] *Pan He,*[†] *and Liqiang Mai*[*,†,∥]

[†]State Key Laboratory of Advanced Technology for Materials Synthesis and Processing, Wuhan University of Technology, Wuhan 430070, People's Republic of China

[‡]College of Science, Huazhong Agricultural University, Wuhan 430070, People's Republic of China

[§]Department of Materials Science and NanoEngineering, Rice University, Houston, Texas 77005, United States

[∥] Department of Chemistry, University of California, Berkeley, California 94720, United States

Corresponding Author

*E-mail: mlq518@whut.edu.cn (L.M.).

*E-mail: luoyanzhu@mail.hzau.edu.cn (Y.L.).

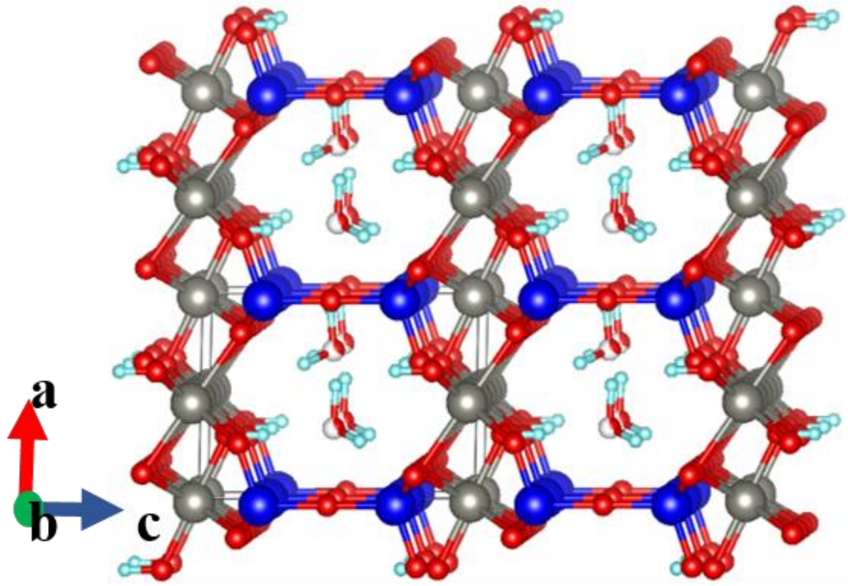

Figure S1. Crystal structure of $Zn_3V_2O_7(OH)_2{\cdot}2H_2O$ (a,b,c refers to the a,b,c axis of crystal cell; grey: Zn; dark blue: V; red: O; light blue: H; molecule in the layers: H_2O;)

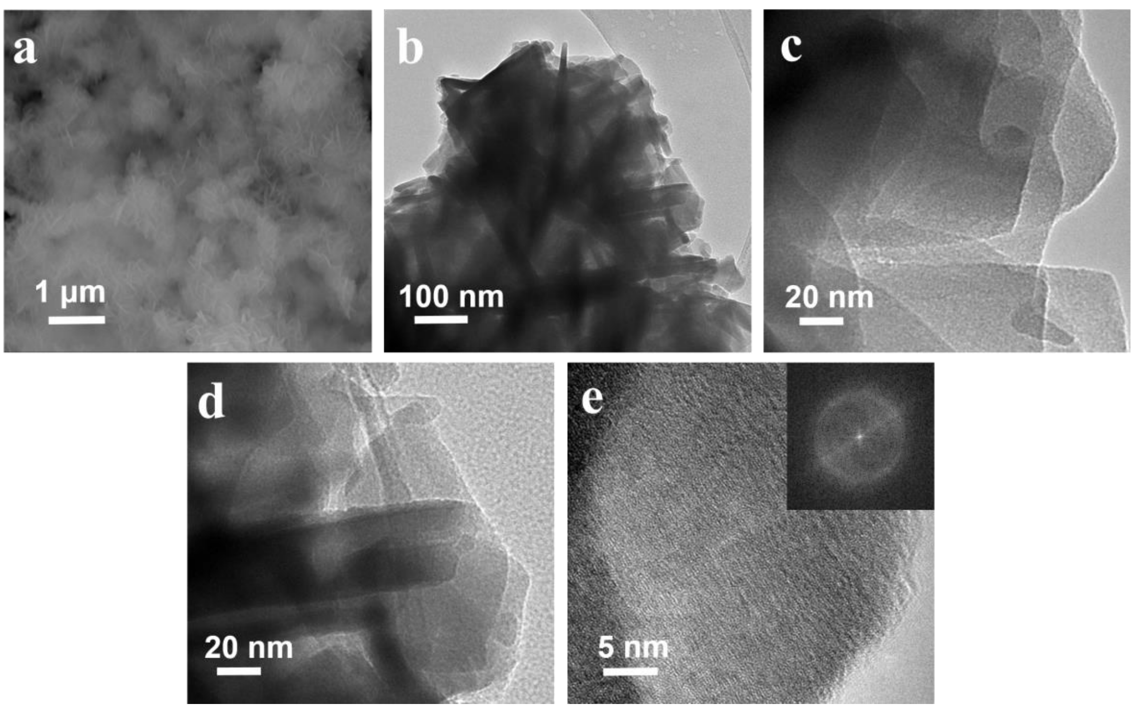

Figure S2. (a) SEM image of ZnVO-2. (b-e) TEM, HRTEM images, and FFT pattern of ZnVO-2.

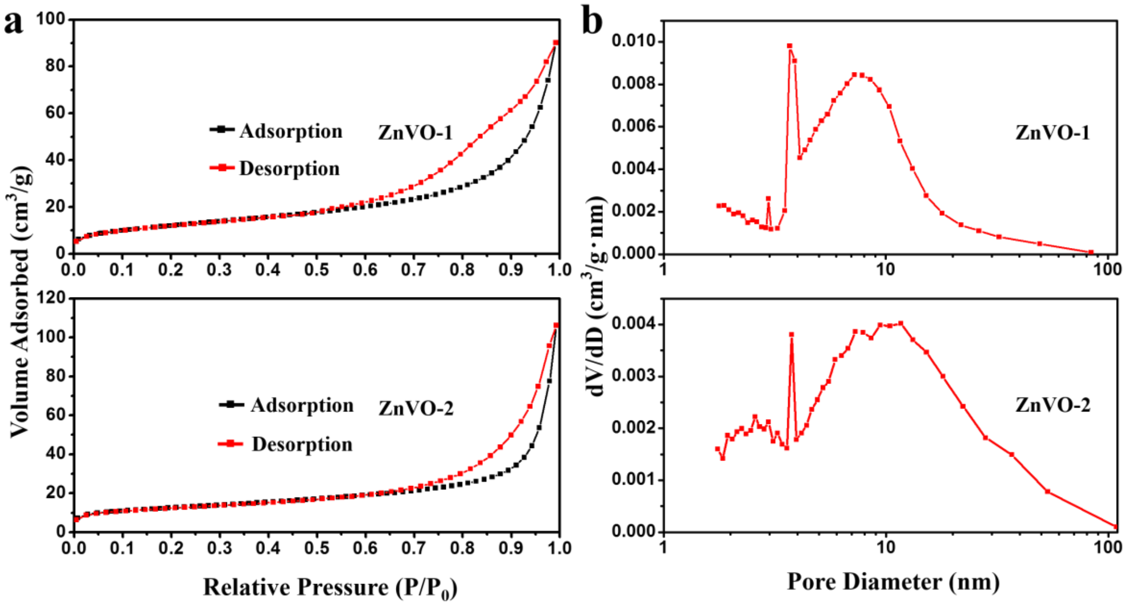

Figure S3. (a) The N_2 adsorption-desorption isotherms of ZnVO-1 and ZnVO-2. (b) The corresponding BJH pore size distribution curves of ZnVO-1 and ZnVO-2.

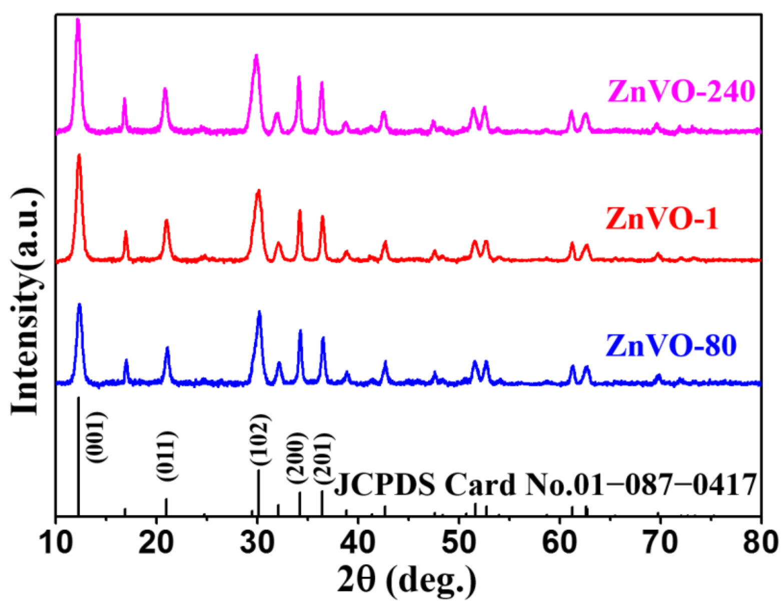

Figure S4. XRD patterns of ZnVO-80, ZnVO-1, and ZnVO-240.

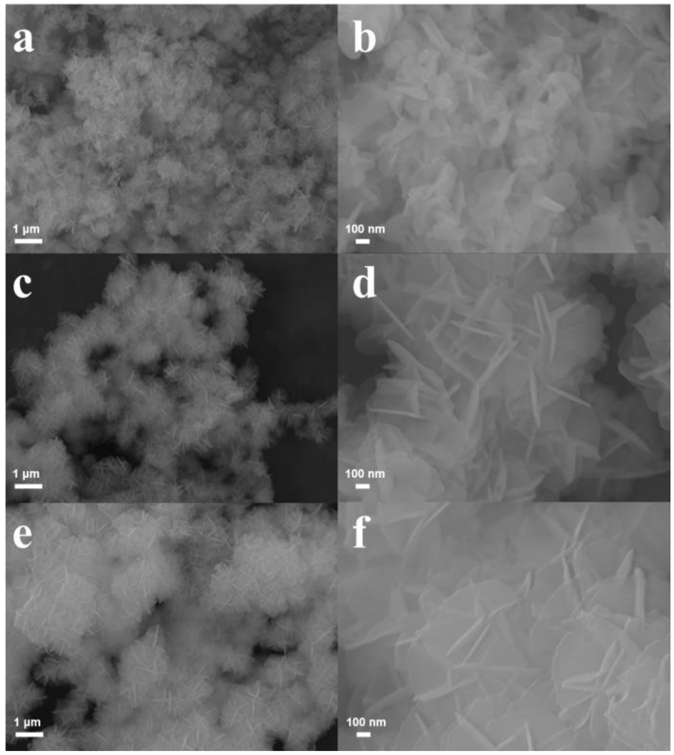

Figure S5. SEM images of (a,b) ZnVO-80, (c,d) ZnVO-1, and (e,f) ZnVO-240.

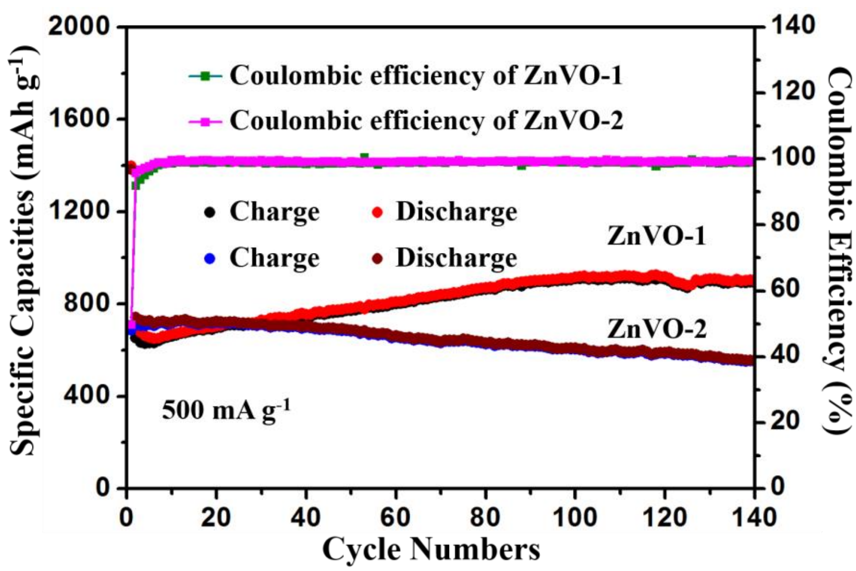

Figure S6. The electrochemical performance of the ZnVO-1 and ZnVO-2 at current density of 500 mA g^{-1}.

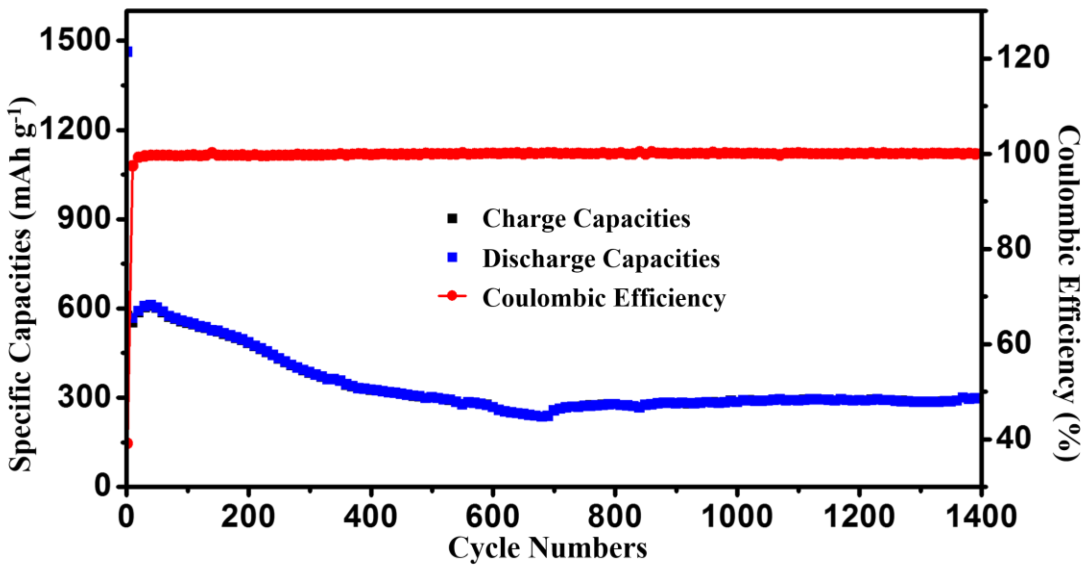

Figure S7. Long cycling performance and corresponding Coulombic efficiency of ZnVO-1 at 5 A g^{-1}.

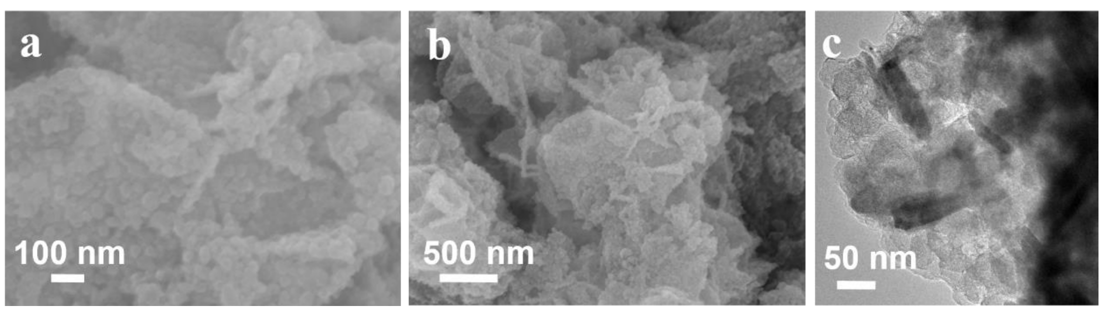

Figure S8. (a, b)SEM images and c)TEM image of the charged-state ZnVO-1 electrode after 100 cycles.

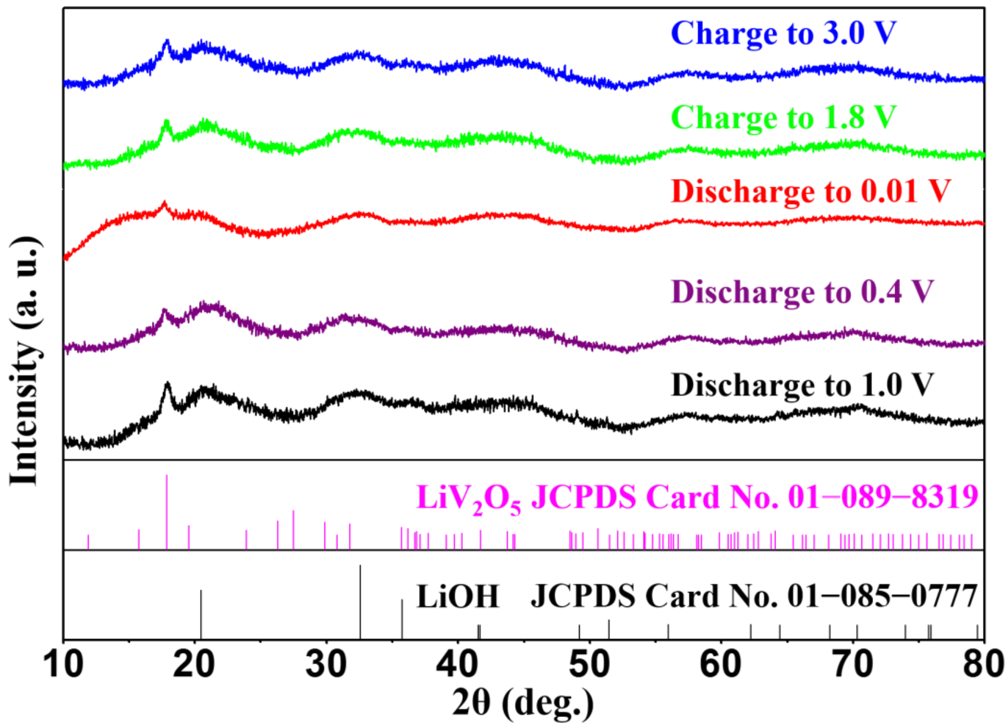

Figure S9. Ex situ XRD patterns of ZnVO-1 electrode at different states in the 30th cycle.

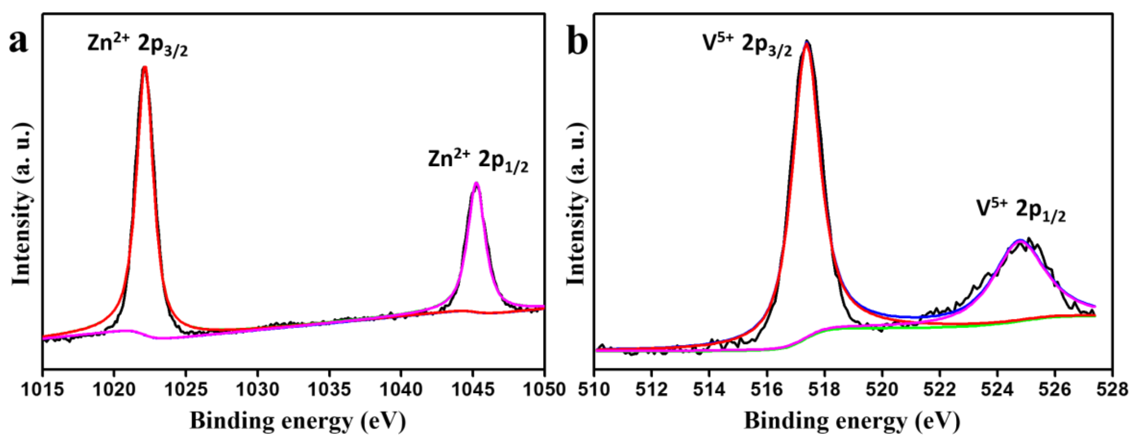

Figure S10. High resolution (a)Zn 2p XPS spectra and (b)V 2p XPS spectrum of fresh ZnVO-1 electrode.

Table S1. Comparison of specific capacities between our work and pervious works

Electrode	Reversible capacity (mA h g^{-1})	Current density (mA g^{-1})	Cycle numbers	Mass ratio	Voltage range (V vs Li^+/Li)
ZnVO-1	**1287**	**200**	**140**	**7:2:1**	**0.01-3**
	931	**500**	**500**	**7:2:1**	**0.01-3**
$Zn_3V_2O_7(OH)_2 \cdot 2H_2O$ graphene network[1]	930	200	200	7:2:1	0.01-3
$Zn_3V_2O_7(OH)_2 \cdot 2H_2O$ nanobelts[2]	750	20	20	7:2:1	0.02-2.5
$Zn_3V_2O_7(OH)_2 \cdot 2H_2O$ 3D microspheres[3]	619	20	20	8:1:1	0.02-2.5
$Zn_3V_2O_8$ nanocages[4]	1400	100	80	6:3:1	0.005-3
$Zn_3V_2O_8$ hexagon nanosheets[5]	1103	200	150	6:3:1	0.01-3
Ultralong monoclinic ZnV_2O_6 nanowires[6]	973	100	10	4.5:5:0.5	0.025-3
$Zn_3V_3O_8$/C microspheres[7]	912	400	150	7:2:1	0.01-3
ZnV_2O_4 microspheres[8]	501	100	100	8:1:1	0.02-3
$Zn_3V_2O_8$ 3D microspheres[3]	492	20	20	8:1:1	0.02-2.5
$Zn_3V_2O_8$ nanoplatelets[9]	270	100	40	8:1:1	0.01-3

The mass ratio in the table refers to the mass ratio of active materials, conducting materials and binder

Reference

(1) Yu, Y.; Niu, C.; Han, C.; Zhao, K.; Meng, J.; Xu, X.; Zhang, P.; Wang, L.; Wu, Y.; Mai, L. Zinc Pyrovanadate Nanoplates Embedded in Graphene Networks with Enhanced Electrochemical Performance. *Ind. Eng. Chem. Res.* **2016,** *55,* 2992–2999.

(2) Zhang, S.; Lei, N.; Ma, W.; Zhang, Z.; Sun, Z.; Wang, Y. Fabrication of Ultralong $Zn_3V_2O_7(OH)_2{\cdot}2H_2O$ Nanobelts and Its Application in Lithium-Ion Batteries. *Mater. Lett.* **2014,** *129,* 91–94.

(3) Zhang, S.; Xiao, X.; Lu, M.; Li, Z. $Zn_3V_2O_7(OH)_2{\cdot}2H_2O$ and $Zn_3(VO_4)_2$ 3D Microspheres as Anode Materials for Lithium-Ion Batteries. *J. Mater. Sci.* **2013,** *48*, 3679–3685.

(4) Yin, Z.; Qin, J.; Wang, W.; Cao, M. Rationally Designed Hollow Precursor-Derived $Zn_3V_2O_8$ Nanocages as a High-Performance Anode Material for Lithium-Ion Batteries. *Nano Energy* **2017,** *31*, 367–376.

(5) Gan, L.; Deng, D.; Zhang, Y.; Li, G.; Wang, X.; Jiang, L.; Wang, C. $Zn_3V_2O_8$ Hexagon Nanosheets: a High-Performance Anode Material for Lithium-Ion Batteries. *J. Mater. Chem. A* **2014,** *2*, 2461–2466.

(6) Sun, Y.; Li, C.; Wang, L.; Wang, Y.; Ma, X.; Ma, P.; Song, M. Ultralong Monoclinic ZnV_2O_6 Nanowires: Their Shape-Controlled Synthesis, New Growth Mechanism, and Highly Reversible Lithium Storage in Lithium-Ion Batteries. *RSC Adv.* **2012,** *2,* 8110–8115.

(7) Bie, C.; Pei, J.; Chen, G.; Zhang, Q.; Sun, J.; Yu, Y.; Chen, D. Hierarchical $Zn_3V_3O_8$/C Composite Microspheres Assembled from Unique Porous Hollow Nanoplates with Superior Lithium Storage Capability. *J. Mater. Chem. A* **2016,** *4*, 17063–17072.

(8) Zheng, C.; Zeng, L.; Wang, M.; Zheng, H.; Wei, M. Synthesis of Hierarchical ZnV_2O_4 Microspheres and Its Electrochemical Properties. *CrystEngComm* **2014,** *16,* 10309–10313.

(9) Vijayakumar, S.; Lee, S. H.; Ryu, K. S. Synthesis of $Zn_3V_2O_8$ Nanoplatelets for Lithium-Ion Battery and Supercapacitor Applications. *RSC Adv.* **2015,** *5,* 91822–91828.